

## Hexagonal boron nitride and 6H-SiC heterostructures

S. Majety, J. Li, W. P. Zhao, B. Huang, S. H. Wei et al.

Citation: *Appl. Phys. Lett.* **102**, 213505 (2013); doi: 10.1063/1.4808365

View online: <http://dx.doi.org/10.1063/1.4808365>

View Table of Contents: <http://apl.aip.org/resource/1/APPLAB/v102/i21>

Published by the [American Institute of Physics](#).

---

### Additional information on *Appl. Phys. Lett.*

Journal Homepage: <http://apl.aip.org/>

Journal Information: [http://apl.aip.org/about/about\\_the\\_journal](http://apl.aip.org/about/about_the_journal)

Top downloads: [http://apl.aip.org/features/most\\_downloaded](http://apl.aip.org/features/most_downloaded)

Information for Authors: <http://apl.aip.org/authors>

## ADVERTISEMENT



Improve your Images with Minus K's  
**Negative-Stiffness** Vibration Isolation

Workstations & Optical Tables



Custom Applications



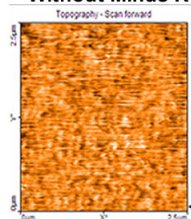
Bench Top Isolators



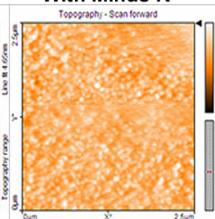
Multi Isolator Systems



Without Minus K



With Minus K



Floor Platforms



## Hexagonal boron nitride and 6H-SiC heterostructures

S. Majety,<sup>1</sup> J. Li,<sup>1</sup> W. P. Zhao,<sup>1</sup> B. Huang,<sup>2</sup> S. H. Wei,<sup>2</sup> J. Y. Lin,<sup>1</sup> and H. X. Jiang<sup>1,a)</sup>

<sup>1</sup>Department of Electrical and Computer Engineering, Texas Tech University, Lubbock, Texas 79409, USA

<sup>2</sup>National Renewable Energy Laboratory, 1617 Cole Boulevard, Golden, Colorado 80401, USA

(Received 24 April 2013; accepted 16 May 2013; published online 31 May 2013)

Hexagonal boron nitride (hBN) epilayers were grown on n-type 6H-SiC substrates via metal organic chemical vapor deposition. X-ray diffraction measurements confirmed that the epilayers are of single hexagonal phase. Photoluminescence (PL) studies revealed a dominant band edge emission at around 5.5 eV, similar to the PL spectra of hBN epilayers grown on sapphire. The current-voltage (I-V) characteristics of the hBN/6H-SiC heterostructure were measured and the results were utilized to determine the band offsets of the hBN/6H-SiC heterojunctions. The analysis yielded the conduction and valence band offsets ( $\Delta E_C$  and  $\Delta E_V$ ) of the hBN/6H-SiC heterointerface of about 2.3 and 0.7 ( $\pm 0.2$ ) eV, respectively, giving a  $\Delta E_C/\Delta E_g$  value of around 76%. The measured band offsets are in reasonable agreement with values deduced from the band alignments between hBN, AlN, and 6H-SiC obtained from independent experimental data and theoretical calculations. © 2013 AIP Publishing LLC. [<http://dx.doi.org/10.1063/1.4808365>]

Hexagonal boron nitride (hBN) has been the material of heavy interest recently due to its unique physical properties, including high thermal conductivity, chemical stability, negative electron affinity, and a large band gap ( $E_g \sim 6$  eV).<sup>1–5</sup> The reported low dielectric constant ( $k$ ) of  $\sim 4$  and high mass density of 1.8–2.0 g/cm<sup>3</sup> coupled with high breakdown field ( $>4.4$  MV/cm for hBN epilayers) and low leakage currents make it a very attractive material for low- $k$  applications.<sup>6–8</sup> With the popularity that graphene has garnered, hBN has also emerged as an ideal template and gate dielectric layer for graphene. Lasing action in the deep UV (DUV) range ( $\sim 225$  nm) has been demonstrated in bulk hBN crystals via e-beam pumping,<sup>5</sup> suggesting that it is a suitable material for DUV photonic device applications. The hexagonal layered structure of hBN increases the exciton binding energy and the optical emission efficiency over 3D systems. Huang *et al.* has recently established through group theory analysis and first principle calculations that the strong band edge emission in hBN originates from the abnormally strong  $p \rightarrow p$  like transition and two-dimensional (2D) nature of hBN.<sup>9</sup> The band edge photoluminescence (PL) intensity of hBN was observed to be two orders of magnitude higher than that of AlN which has a comparable band gap as hBN.<sup>7</sup> The wafer scale growth of good quality hBN epilayers could potentially make it the material of choice for DUV photonic devices which relied heavily on AlN till now. The ability to dramatically reduce the p-type resistivity of hBN by Mg doping is another huge advantage over AlN and suggests the possibility of achieving DUV optoelectronic devices with high quantum efficiency.<sup>10</sup>

To expand our epitaxial growth studies beyond hBN on sapphire substrates and AlGaN templates,<sup>7,10–12</sup> here we report on the synthesis of good quality hBN epilayers on highly conductive n-type 6H-SiC (0001) substrates. Previous studies on the growth of hBN layers were mostly confined to sapphire, Ni(111), and silicon substrates with very limited reports on the growth of hBN on SiC substrates.<sup>13,14</sup> The

semiconducting properties of hBN/SiC heterostructures have not been previously studied and are expected to open up opportunities to design electronic and photonic devices with very interesting applications.

Undoped hBN epilayers of thickness  $\sim 0.5$   $\mu\text{m}$  were grown using low pressure metal organic chemical vapor deposition (MOCVD). The precursors for boron and nitrogen are triethyl-boron (TEB) and ammonia (NH<sub>3</sub>), respectively. The growth was carried out on n-type 6H-SiC (0001) on-axis substrates. The (0001) surface of SiC is the Si terminated surface. The electrical resistivity of the 6H-SiC substrate is around 0.01  $\Omega\text{cm}$  with a free electron concentration around  $5 \times 10^{18}$  cm<sup>-3</sup>. The growth of hBN was carried out using hydrogen (H<sub>2</sub>) as a carrier gas to transport the pre-cursors. The growth temperature of hBN epilayers was 1300 °C with a low temperature buffer of BN incorporated at 800 °C. Due to the crystal structure mismatch between hBN and 6H-SiC (in-plane lattice constants 2.5 Å and 3.08 Å, respectively), prior to epilayer growth, a 20 nm BN buffer layer was first deposited on 6H-SiC substrate at 800 °C. Similar to the case in the conventional III-nitride epitaxial growth, the functions of this buffer layer include providing strain relieve from lattice mismatch between the substrate and the subsequent hBN epilayer. Furthermore, it was found that the use of the buffer layer enhances significantly the adhesion of hBN epilayers to the substrates. The schematic of the hBN/n-SiC heterostructure is shown in the inset of Fig. 1. X-ray diffraction (XRD) was used to investigate the crystalline quality and lattice constant of the hBN layers. PL studies were conducted on these samples using our deep UV laser spectroscopy setup. The excitation laser with a photon energy set at 6.3 eV for PL measurements was obtained through the fourth harmonic generation of femtosecond version of Ti:Sapphire laser. PL signal was dispersed using a 1.3 m monochromator and detected by a photo-multiplier tube (PMT).<sup>15</sup>

Figure 1 shows the XRD  $\theta$ - $2\theta$  scan of the hBN/6H-SiC heterostructure with a hBN (0002) reflection peak at 26.5°.

<sup>a)</sup>hx.jiang@ttu.edu

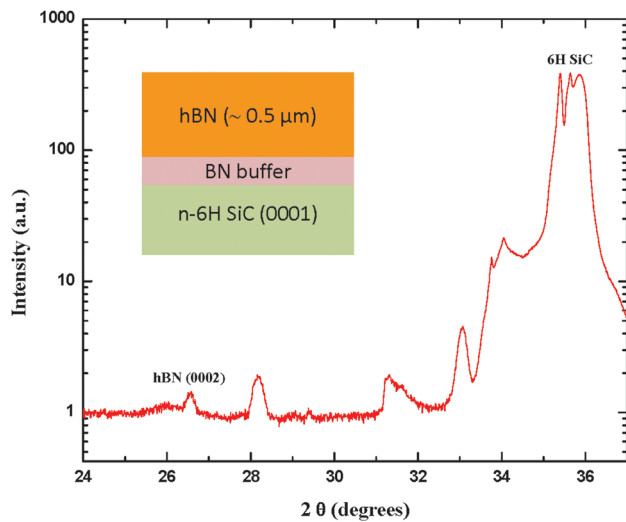


FIG. 1. XRD  $\theta$ - $2\theta$  scan of hBN/6H SiC revealing the position of the hBN (0002) reflection peak at  $26.5^\circ$ . The inset shows the layer structure of hBN/6H-SiC heterostructures.

This yields a corresponding lattice constant of  $c = 6.70 \text{ \AA}$ , which closely matches hBN bulk crystal lattice constant of  $c = 6.66 \text{ \AA}$ .<sup>16,17</sup> No other diffraction peaks were observed from hBN indicating that the hBN epilayers are of single hexagonal phase. The other peaks were present in the original XRD pattern from the SiC substrate before epitaxy and are not associated with hBN film. XRD intensity of the hBN (002) peak indicates that the crystalline quality of these epilayers grown on 6H-SiC are not as good as hBN grown on sapphire or AlN.<sup>10-12</sup> We believe that further optimization of growth parameters will yield comparable results.

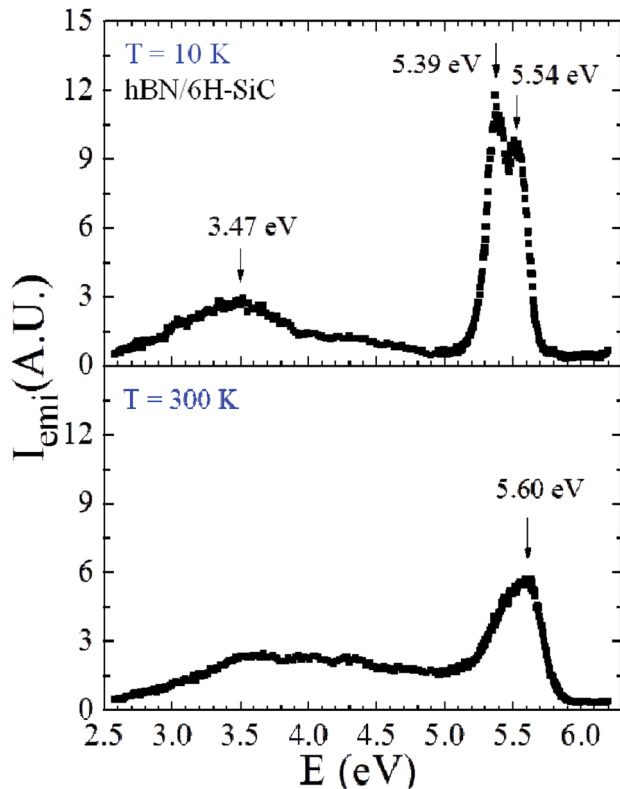


FIG. 2. Photoluminescence spectra of hBN on n-type 6H-SiC measured at 10 K (top) and 300 K (bottom).

Room temperature (300 K) and low temperature (10 K) PL spectra for hBN epilayers grown on 6H-SiC are shown in Fig. 2. These PL spectra show a dominant band edge related emission at  $\sim 5.5 \text{ eV}$ , consistent with the PL spectra of hBN epilayers grown on sapphire.<sup>10,11</sup> At 10 K, the dominant emission band resolved into two emission peaks at  $5.54 \text{ eV}$  and  $5.39 \text{ eV}$ . A broad impurity transition at  $3.47 \text{ eV}$  was also observed. The nature of such an impurity transition is not clear at this point.

The conduction band offset ( $\Delta E_C$ ) is the fundamental parameter of a heterostructure system. One of the most direct measurement techniques for determining  $\Delta E_C$  is based on the analysis of current-voltage ( $I$ - $V$ ) characteristics of the heterostructure itself.<sup>18</sup> Ohmic contacts with a cross section area of about  $9 \text{ mm}^2$  consisting of Ni (30 nm)/Au (120 nm) bilayer were deposited on the hBN surface. Thermal treatment (rapid thermal annealing) at  $1020^\circ \text{C}$  of the Ni/Au/hBN contacts in a  $\text{N}_2$  ambient atmosphere was used to decrease the contact resistance and enhance the Ohmic behavior of these contacts.<sup>12</sup> The sample was etched down to the n-SiC layer using inductively coupled plasma dry etching and n-contacts consisting of a layer of Ni (100 nm) were deposited in n-SiC. For the n-contacts to SiC, annealing in a  $\text{N}_2$  ambient at  $950^\circ \text{C}$  for 100 s produced Ohmic contacts. Separate measurements were carried out to confirm the Ohmic behavior of the Ni/Au/hBN and the Ni/n-SiC contacts. The inset of Fig. 3(a) depicts the schematic layout of the structure with Ohmic contacts on hBN (Ni/Au) and n-SiC (Ni).

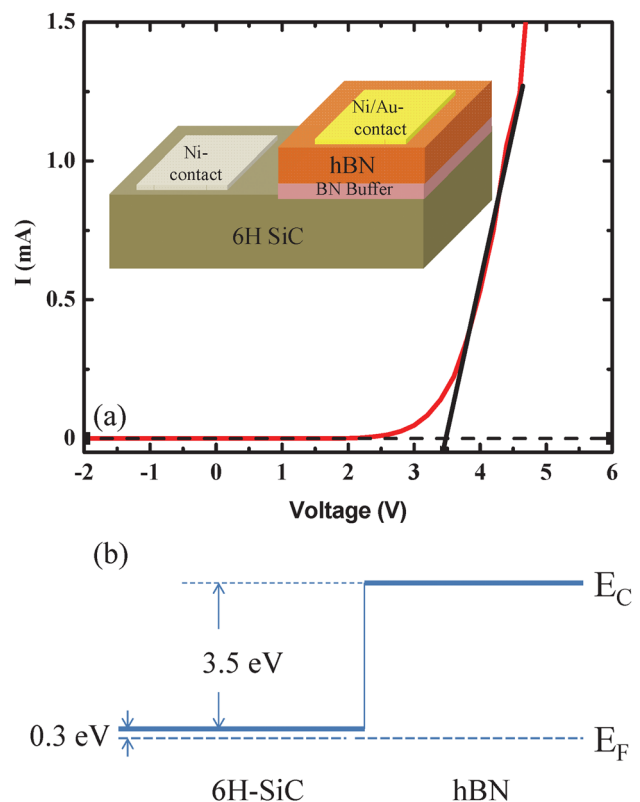


FIG. 3. (a)  $I$ - $V$  characteristics of an hBN/n-6H-SiC heterostructure. The inset is a schematic diagram of the heterostructure used for the measurements. (b) The conduction band alignment between hBN and n-type 6H-SiC deduced from the  $I$ - $V$  characteristics of the heterostructure.

Figure 3(a) shows the I-V characteristics of hBN/n-SiC heterostructures. A rectifying behavior was observed. Due to large bandgap difference between 6H-SiC and hBN, thermionic emission of electrons over the hBN barrier can be neglected. A sharp increase in current occurs when the applied voltage is at the onset to produce a flat band condition across the heterointerface. The extrapolation of the I-V characteristics to  $I=0$  provides the magnitude of the built-in voltage at the heterointerface,<sup>18</sup>  $V_o$ . The estimated voltage drop across the hBN epilayer is around 0.1 V and can be neglected since the expected magnitude of the experimental uncertainty is around  $\pm 0.2$  V and hence  $V_o$  represents a direct measure of the band offset for the hBN/n-SiC heterostructures. Based on the measured built-in voltage ( $V_o \sim 3.5$  V) from Fig. 3(a), we obtain a conduction band alignment for the n-type 6H-SiC and undoped hBN heterointerface by taking the Fermi level in n-type 6H-SiC to be 0.3 eV below the conduction band edge,<sup>19</sup> as illustrated in Fig. 3(b). Based on the results presented in Fig. 3, we can further deduce the band alignment for the intrinsic 6H-SiC/hBN heterostructures by recognizing that the Fermi levels in 6H-SiC and hBN lineup in the middle of the bandgaps in intrinsic materials, as depicted in Fig. 4(a). In constructing Fig. 4(a), we take the band gaps of 6H-SiC and hBN to be around 3.0 and 6.0 eV, respectively. From Fig. 4(a), it can be seen that valence and conduction band offsets are  $\Delta E_V \sim 0.7 \pm 0.2$  eV and  $\Delta E_C \sim 2.3 \pm 0.2$  eV, respectively, giving the ratio of  $\Delta E_C/\Delta E_g \approx 76\%$ . The result shown in Fig. 4(a) implies that 6H-SiC/hBN is a type I (straddling gap) heterojunction.

There have been no reports of theoretical or measured value of  $\Delta E_C$ , which could shed light on the band offsets at the interface of 6H-SiC and hBN heterojunction. There have, however, been experimental measurements that have been validated by theoretical calculations on the band alignment between AlN and 6H-SiC, which yielded a conduction band

offset of about 1.9 eV.<sup>20</sup> We have calculated the band offsets between hBN and AlN using first principles calculations, which suggest that it is a type II (staggered gap) band alignment with  $\Delta E_V = 0.67$  eV and  $\Delta E_C = 0.57$  eV. Using these independent data, we have constructed the band alignments between hBN, 6H-SiC and AlN, as shown in Fig. 4(b), from which a conduction band offset ( $\Delta E_C$ ) of about 2.47 eV is deduced for the 6H-SiC/hBN heterojunction. This value of  $\Delta E_C$  (2.47 eV) obtained from independent experimental data<sup>20</sup> and first-principles calculations agrees reasonably well with the value of  $2.3 \pm 0.2$  eV shown in Fig. 4(a) deduced experimentally from the analysis of I-V characteristics of hBN/6H-SiC heterostructures.

One of the important implications of the calculated band alignment between hBN and AlN is the great potential of hBN for DUV photonics device applications. Due to the fact that the valence band of hBN lies  $\sim 0.67$  eV above that of AlN and ability for p-type conductivity control via Mg doping,<sup>10</sup> hBN would be superior over AlN as an electron blocking and hole injection layer for the construction of DUV emitters and potentially provides a revolutionary p-layer approach to overcome the intrinsic problem of low p-type conductivity (or low free hole concentration) in Al-rich AlGaN.<sup>10,12</sup>

In summary, hBN epilayers were grown on n-type 6H-SiC substrates using low pressure MOCVD and characterized by XRD, PL, and I-V measurements. The band offset of 6H-SiC and hBN heterostructure has been deduced to be  $\Delta E_C/\Delta E_g \approx 76\%$  from the I-V characteristics analysis, which is in reasonable agreement with calculations.

We acknowledge the assistance of PL measurement by X. K. Cao. The device fabrication effort is supported by DHS ARI Program (2011-DN-077-ARI048) and the measurements and data analysis efforts for the band offset determination are supported by DOE (DE-FG02-09ER46552). Jiang and Lin are grateful to the AT&T Foundation for the support of Ed Whitacre and Linda Whitacre Endowed chairs.

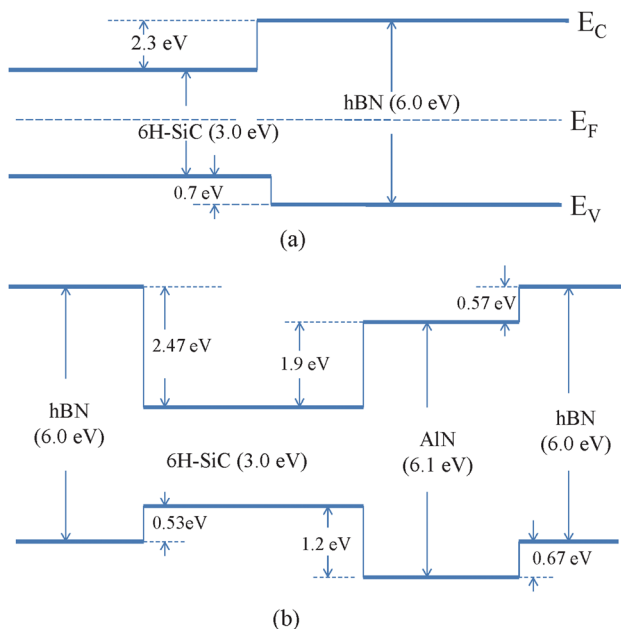


FIG. 4. (a) Band alignment between intrinsic 6H-SiC and hBN deduced from the I-V characteristics of the heterostructures of Fig. 3. (b) Band alignments between intrinsic hBN, 6H-SiC, and AlN constructed from independent experimental data for AlN/6H-SiC heterojunction in Ref. 20 and the first principles calculations for hBN/AlN heterojunction.

<sup>1</sup>Y. Kubota, K. Watanabe, O. Tsuda, and T. Taniguchi, *Science* **317**, 932 (2007).

<sup>2</sup>T. Sugino, C. Kimura, and T. Yamamoto, *Appl. Phys. Lett.* **80**, 3602 (2002).

<sup>3</sup>D. Pacilé, J. C. Meyer, Ç. Ö. Girit, and A. Zettl, *Appl. Phys. Lett.* **92**, 133107 (2008).

<sup>4</sup>L. Song, L. Ci, H. Lu, P. B. Sorokin, C. Jin, J. Ni, A. G. Kvashnin, D. G. Kvashnin, J. Lou, B. I. Yakobson, and P. M. Ajayan, *Nano Lett.* **10**, 3209 (2010).

<sup>5</sup>K. Watanabe, T. Taniguchi, and H. Kanda, *Nat. Photonics* **3**, 591 (2009).

<sup>6</sup>A. J. Gatesman, R. H. Giles, and J. Waldman, *Proc. MRS* **242**, 623 (1992).

<sup>7</sup>J. Li, S. Majety, R. Dahal, W. P. Zhao, J. Y. Lin, and H. X. Jiang, *Appl. Phys. Lett.* **101**, 171112 (2012).

<sup>8</sup>S. W. King, M. French, J. Bielefeld, M. Jaehnig, M. Kuhn, and B. French, *Electrochem. Solid-State Lett.* **14**, H478 (2011).

<sup>9</sup>B. Huang, X. K. Cao, H. X. Jiang, J. Y. Lin, and S. H. Wei, *Phys. Rev. B* **86**, 155202 (2012).

<sup>10</sup>R. Dahal, J. Li, S. Majety, B. N. Pantha, X. K. Cao, J. Y. Lin, and H. X. Jiang, *Appl. Phys. Lett.* **98**, 211110 (2011).

<sup>11</sup>S. Majety, J. Li, X. K. Cao, R. Dahal, B. N. Pantha, J. Y. Lin, and H. X. Jiang, *Appl. Phys. Lett.* **101**, 051110 (2012).

<sup>12</sup>S. Majety, J. Li, X. K. Cao, R. Dahal, B. N. Pantha, J. Y. Lin, and H. X. Jiang, *Appl. Phys. Lett.* **100**, 061121 (2012).

<sup>13</sup>Y. Kobayashi, T. Nakamura, T. Akasaka, T. Makimoto, and N. Matsumoto, *J. Cryst. Growth* **298**, 325 (2007).

<sup>14</sup>Y. Kobayashi and T. Akasaka, *J. Cryst. Growth* **310**, 5044 (2008).

- <sup>15</sup>K. B. Nam, J. Li, M. L. Nakarmi, J. Y. Lin, and H. X. Jiang, *Appl. Phys. Lett.* **84**, 5264 (2004).
- <sup>16</sup>S. L. Rumyantsev, M. E. Levinshtein, A. D. Jackson, S. N. Mohammad, G. L. Harris, M. G. Spencer, and M. S. Shur, in *Properties of Advanced Semiconductor Materials GaN, AlN, InN, BN, SiC, SiGe*, edited by M. E. Levinshtein, S. L. Rumyantsev, and M. S. Shur (John Wiley and Sons, Inc., New York, 2001), pp. 67–92.
- <sup>17</sup>R. W. Lynch and H. G. J. Drickamer, *J. Chem. Phys.* **44**, 181 (1966).
- <sup>18</sup>S. L. Feng, J. Krynicki, V. Donchev, J. C. Bourgoin, M. Di Forte-Poisson, C. Brylinski, S. Delage, H. Blanck, and S. Alaya, *Semicond. Sci. Technol.* **8**, 2092 (1993).
- <sup>19</sup>Z. Sitar, M. J. Paisley, D. K. Smith, and R. E. Davis, *Rev. Sci. Instrum.* **61**, 2407 (1990).
- <sup>20</sup>J. Choi and J. P. Chang, *J. Appl. Phys.* **98**, 093513 (2005).